ISPRS Journal of Photogrammetry and Remote Sensing 65 (2010) 77–85

Contents lists available at ScienceDirect

ISPRS Journal of Photogrammetry and Remote Sensing

journal homepage: www.elsevier.com/locate/isprsjprs

Statistical information of ASAR observations over wetland areas: An interaction model interpretation

F. Grings [a,*], M. Salvia [a], H. Karszenbaum [a], P. Ferrazzoli [b], P. Perna [a], M. Barber [a], J. Jacobo Berlles [c]

[a] Instituto de Astronomía y Física del Espacio (IAFE), Ciudad Universitaria, 1428 Buenos Aires, Argentina

[b] Università di Roma "Tor Vergata", Facoltà di Ingegneria, Dipartimento di Informatica, Sistemi e Produzione (DISP), Via del Politecnico 1, 00133 Roma, Italy

[c] Universidad de Buenos Aires, Facultad de Ciencias Exactas y Naturales (FCEyN), Dpto. de Computación - Ciudad Universitaria, Pab. I, 1428 Buenos Aires, Argentina

ARTICLE INFO

Article history:
Received 30 January 2008
Received in revised form
7 August 2009
Accepted 25 August 2009
Available online 15 September 2009

Keywords:
Statistics
SAR
Ecology
Floods
Hydrology

ABSTRACT

This paper presents the results obtained after studying the relation between the statistical parameters that describe the backscattering distribution of *junco* marshes and their biophysical variables. The results are based on the texture analysis of a time series of Envisat ASAR C-band data (APP mode, VV + HH polarizations) acquired between October 2003 and January 2005 over the Lower Paraná River Delta, Argentina. The image power distributions were analyzed, and we show that the *K* distribution provides a good fitting of SAR data extracted from wetland observations for both polarizations. We also show that the estimated values of the order parameter of the *K* distribution can be explained using fieldwork and reasonable assumptions. In order to explore these results, we introduce a radiative transfer based interaction model to simulate the *junco* marsh σ^0 distribution. After analyzing model simulations, we found evidence that the order parameter is related to the *junco* plant density distribution inside the *junco* marsh patch. It is concluded that the order parameter of the *K* distribution could be a useful parameter to estimate the *junco* plant density. This result is important for basin hydrodynamic modeling, since marsh plant density is the most important parameter to estimate marsh water conductance.

1. Introduction

Areas near rivers, or in low-lying coastal places, are in risk of flooding. Periods of heavy rain, not necessarily in the area, can lead to increases in the water level of streams and rivers to a point where the main channels can no longer hold the volume of incoming water. In wetland areas, it is claimed that this excess of water can be taken by marshes located in the floodplain separated from the mainstream channel by island levees. These marshes are continuously exchanging water with the mainstream channel, but in extreme flood conditions, when the river overflows, the net flux goes in the marsh direction (Arihood and Sidle, 2006). When the river water level returns to normal, this excess of water moves back to the mainstream channel. This capability is usually called the "marsh buffer effect" because its effect is analogous to a low pass filter that "smoothes" the mainstream flux (Novitzki and Fretwell, 2002).

In the Lower Delta of the Paraná River in Argentina, marshes are the most extended autochthonous vegetation. The species that dominates the marsh vegetation is the *junco* marsh (*Schoenoplectus californicus*), and it covers up to 25% of the wetland area (~800 km^2). These marshes are mainly located in islands along the channels and they are responsible for the water buffer effect on this wetland.

Water storage in floodplains is also a governing parameter in continental scale hydrologic models (Keedy, 2000). Coe (2000) reported that a wetland component could provide up to 50% of the observed Nile River discharge in the Sudan. Furthermore, Richey et al. (1989) estimated that the Amazon floodplain-to-mainstream flux is about 25% of the annual discharge. These large percentages suggest that inaccurate knowledge of floodplain storage and discharge can lead to significant errors in hydrological models (Alsdorf, 2002).

In order to characterize this buffer effect, there are two important magnitudes to be estimated: the marsh water storage capacity and the marsh hydraulic conductivity. Marsh water storage capacity determination consists of the estimation of the volume of water inside wetland islands; this can be done using remote sensing data in several ways (Alsdorf, 2002; Coe, 2000; Keedy, 2000) and it has been estimated previously on the Paraná River wetland for flooded and non-flooded conditions using both field

* Corresponding address: Instituto de Astronomía y Fisica del Espacio (IAFE), CC 67 - Suc. 28, (C1428ZAA) Ciudad Autonoma de Buenos Aires, Argentina. Tel.: +54 7890179; fax: +54 47868114.

E-mail addresses: verderis@iafe.uba.ar (F. Grings), ferrazzoli@disp.uniroma2.it (P. Ferrazzoli), jacobo@dc.uba.ar (J. Jacobo Berlles).

0924-2716/$ – see front matter © 2009 International Society for Photogrammetry and Remote Sensing, Inc. (ISPRS). Published by Elsevier B.V. All rights reserved.
doi:10.1016/j.isprsjprs.2009.08.003

data and Envisat ASAR images (Grings et al., 2006, 2008, 2009). Characterization of hydraulic conductivity is a much more difficult task, which requires the estimation of the drag coefficient of the vegetation in different areas of the watershed (Järvelä, 2004a). Nevertheless, many authors have pointed out that the vegetation drag coefficient in herbaceous vegetation ecosystems (like *junco* marshes) depends mostly on the plant density (Järvelä, 2004a; Nepf and Koch, 1999; Stone and Hung, 2002). As a result, the estimation of *junco* plant density information at high spatial resolution and at a regional scale is critical in the hydrodynamic modeling of wetlands.

It was found that the mean σ^0 of a homogenous marsh area is mostly related to a few marsh biogeophysical variables (Grings et al., 2005, 2006, 2008). The question we address in this work is: is there other substantial information that is available in the marsh SAR image? In wetlands, it is common that inside a patch dominated by a single marsh species (homogeneous in terms of species), different marsh *conditions* are present. In the Paraná River Delta, these different conditions of the marsh are usually related to a non-homogeneous distribution of some biogeophysical variables, typically related to the different availability of water and nutrients. Therefore, it is reasonable to assume that some of the variability that is observed in an SAR image of a wetland patch may be related to spatial inhomogeneities of one or more of the main biogeophysical variables that determine the observed σ^0. This idea has already been addressed, and is the base of the interpretation of complex SAR image statistics of inhomogeneous targets (Oliver and Quegan, 1998). Moreover, it has been shown that most of the observed statistics can be interpreted as generated by two unrelated processes encapsulated in a product model (Oliver and Quegan, 1998). This product model states that the observed SAR image is the result of the product of the target backscatter with a speckle component. One underling hypothesis of the multiplicative model is that the parameters characterizing the backscattering distribution are related in some way to target parameters (Blacknell, 1994; Oliver and Quegan, 1998). The problem is that there is no general relation between the statistical distribution of SAR data and the underlying physical interaction between the wave and the ecosystem patch.

This hypothesis was further investigated recently (Wang and Ouchi, 2005). Data acquired over a forest by PI-SAR were fitted to a K distribution, and one of the estimated parameters was associated to the forest biomass. In (Wang and Ouchi, 2005), the authors demonstrated that there is a strong positive correlation between the K homogeneity parameter and the forest biomass, showing that there is some kind of relation between the statistical parameters that characterize forest patches and some of the biogeophysical variables of the terrain (biomass in this case). Furthermore, they also provided a sound speculative interpretation of this relation, which will be explored further in the present paper.

In this work, the SAR image power distributions of *junco* marshes were analyzed, and we show that the K distribution provides a good fitting of SAR data for both HH and VV polarization. We also show that the estimated values of the order parameter of the K distribution are related to the *junco* plant density distribution. Taking up the ideas in Lee et al. (1994); Oliver and Quegan (1998); Wang and Ouchi (2005), we modeled the SAR return of the *junco* marsh to show that there is biophysical information in all the statistical parameters that characterize a given marsh area.

The paper is structured as follows. In Section 2, we introduce the statistical model of SAR backscattering. In Section 3, we illustrate the method adopted to estimate the distribution parameters. In Section 4, we show the results obtained by analyzing an Envisat ASAR time series acquired over the lower Delta of the Paraná River for both HH and VV polarizations. In Section 5, we give a theoretical interpretation of the statistical model by using an interaction model of the marsh area based on radiative transfer theory. In Section 6, we discuss the results obtained in Section 4 taking into account the theoretical results developed in Section 5. Finally, in Section 7 we show a comparison between the statistical parameters estimated from ASAR images and simulated ones.

2. The statistical model

A multiplicative model is commonly adopted for SAR image interpretation (Oliver and Quegan, 1998). This model assumes that the observed intensity value in every pixel is the outcome of a random variable Z, defined as the product between the random variables X and Y, where X represents the random variable modeling the variations of terrain scattering properties and Y represents the random variable modeling the speckle; i.e. $Z = X \cdot Y$. Different distributions for X and for Y yield different models for the observed data Z. For homogeneous regions, the terrain scattering properties are constant. Therefore, the distribution of Z is a rescaled version of the distribution of Y, which is usually assumed, for intensity, as Gamma distributed with parameters $(n, 2n)$. In conventional notation, $Y \sim \Gamma(n, n)$, where n is the *equivalent number of looks* of the SAR image (Oliver and Quegan, 1998).

The basic hypothesis that governs the modeling of inhomogeneous regions is that their scattering properties are not constant, though they can be modeled by a convenient distribution. In this work, it will be assumed that $X \sim \Gamma(\alpha, \beta)$, where α is the shape or homogeneity parameter and β is the scale parameter. This assumption is not arbitrary, since Jakeman and Pusey (1976) show that an inhomogeneous SAR sample in which the number of scatterers per pixel N is itself a random variable distributed inverse binomial will present a Gamma distribution. In this way, this model includes two sources of image inhomogeneity: target spatial variability and speckle; the target variability is related to a fluctuation in the number of scatterers inside every pixel (Jakeman and Pusey, 1976).

The K-distribution model for a radar clutter arises (Oliver and Quegan, 1998) when a Gamma-distributed noise process modulates a Gamma-distributed radar cross-section. It is important to remark on an assumption of this model, which needs to be checked in order to be used: the fluctuation of the target scattering properties should have a greater spatial scale than the speckle, so that multilooking reduces the speckle without affecting the scattering fluctuations (Oliver and Quegan, 1998).

3. Estimation of the parameters of the intensity K distribution

The parameters that define a K distribution can be estimated in several ways (Blacknell, 1994; Frery et al., 1997; Lee et al., 1994; Oliver and Quegan, 1998; Yanasse et al., 1994). In this work we choose the straightforward estimation scheme presented in (Lee et al., 1994). The estimator of β based on the first sample moment of the data $X = \{x_1, x_2, \ldots, x_n\}$ is

$$\hat{\beta} = \frac{1}{N}\sum_{i=0}^{N} X_i = \hat{m}_1. \tag{1}$$

This gives the sample mean. In order to obtain the moment's estimator of α it is necessary to use other moments of the measured distribution (1/2, 2, etc.). One estimator for α using the moment method is

$$\hat{\alpha} = \frac{\hat{m}_{1^2}(n+1)}{n\,(\hat{m}_2 - \hat{m}_{1^2}) - \hat{m}_{1^2}}. \tag{2}$$

To estimate the variances of the parameters, we use the *bootstrapping* method (Cribari-Neto et al., 2002). This method consist of the estimation of the parameter (i.e. β), using a sub-sample X_k

Table 1
Envisat ASAR images used.

Mode	Polarization	Date	Season
APP S1	VV/HH	16/10/2003	Spring
APP S1	VV/HH	20/11/2003	Spring
APP S1	VV/HH	04/03/2004	Summer
APP S1	VV/HH	08/04/2004	Autumn
APP S1	VV/HH	13/05/2004	Autumn
APP S1	VV/HH	09/12/2004	Spring
APP S1	VV/HH	13/01/2005	Summer

consisting of all the available data except the value in the k-position,

$$X_k = X - x_k$$
$$\hat{\beta}_k = \sum_{k=0}^{N-1} X_k = \hat{m}_{1,k}. \quad (3)$$

Then, the variance of the parameter (i.e. β) is estimated as

$$Var(\hat{\beta}) = \frac{1}{N}\sum_{j=0}^{N-1}\left(\hat{\beta}_j - E(\hat{\beta})\right)^2. \quad (4)$$

For the ASAR dataset considered by us (see the next section), the procedure followed for the estimation of the K parameters of a given area was the following:

1. Selection of a known region within the SAR image where fieldwork was available, corresponding to *junco* marshes (*Schoenoplectus californicus*) and willow forest (*Salix* spp).
2. Extraction of the pixel values for different polarizations.
3. Decorrelation of the samples by eliminating all the pixels nearer the overall correlation length (in fact the used model is only valid for decorrelated samples).
4. Computation of the estimated moments of the distribution.
5. Estimation of α, β.
6. Estimation of Kolmogorov statistics using the parameters estimated in step 5, in order to check if a sample was distributed as $K(\alpha, \beta, n)$.

4. Statistical analysis of ASAR data

This study uses a time series of Envisat ASAR precision image products in Alternating Polarization mode (APP). For each date, there is a multilook ground range digital image. The raw data are acquired in bursts of alternating polarizations. The polarization combination used is the co-polarized sub-mode (one image HH and one image VV). Table 1 lists the 7 acquisitions (14 ASAR images, all APP S1 mode – 19° incidence angle) that were processed and analyzed for this work.

For *junco* marsh, radar signatures were collected for both polarizations and for several flood conditions, as we verified by detailed fieldwork, which was carried out simultaneously with Envisat data acquisitions (Fig. 1).

A rigorous and systematic characterization of the target made it possible to analyze the statistical distribution of target parameters. The extraction of quantitative information from multitemporal radar images involved several tasks. ESA BEST software was used for calibration of the alternating polarization data. After calibration, several *junco* and forest samples were extracted from the calibrated ASAR images. Some representative *junco* backscattering samples are shown in Fig. 2.

To obtain the parameters that characterize these distributions, the procedure described in Section 3 was followed. Table 2 shows the estimated values of α and β parameters for all the ASAR acquisitions dates, polarizations and vegetation types. The last column shows the acceptance or rejection of the experimental sample distributions as $K(\alpha, \beta, n)$, using the Kolmogorov test with a probability of 5%.

It is well known that β (the mean of the sample) is a good estimator of the mean σ^0 of the area for a backscattering distributed as $Y \sim \Gamma(\alpha, \beta)$ (Lee et al., 1994). The α parameter, known as the shape parameter, is usually interpreted as the grade of homogeneity of the σ^0 of the area (Oliver and Quegan, 1998). It is important to note that the homogeneity measured by the α parameter is due to real spatial variations of the σ^0 of the extended target. The variability related to the speckle phenomenon is taken into account in the parameter n.

Samples from five images were rejected, since they could not be considered as distributed $K(\alpha, \beta, n)$, according to the Kolmogorov test. All these images correspond to acquisition dates where extreme environmental conditions were observed: a drought in January 2005 and flooding in October and November 2003. In these extreme environmental conditions, the interaction mechanism that characterizes vegetation changes. In these cases, the variance of the α estimator is very large, and no inference can be made from the data.

In Table 2, the estimated values of the β parameter are shown. As we mentioned before, these values are related to the average σ^0 of the area. It can be seen that the values are relatively constant for the forest samples for both HH and VV polarizations. For the *junco*, the HH values are systematically higher than the VV values, and this difference is strongly amplified in the case of flooding (October and November 2003) as we have already shown in Grings et al. (2006). The fact that the images corresponding to flooding events cannot be considered as K distributed does not invalidate this statement, since the sample mean is still a meaningful estimator of the mean power.

Also in Table 2, estimated values of the α parameter are shown. It can be seen that there is a wide dynamic range of values, ranging from ∼20 to near 2. These values should be a measure of the spatial inhomogeneity of σ^0 of the area. From Table 2, two main conclusions can be extracted:

1. Generally, forest samples present a higher α value than *junco* samples for both polarizations.
2. Generally, VV polarization presents a higher α value than HH polarization for both vegetation types.

These two general observations have an important relation with the results reported in Wang and Ouchi (2005). In that paper, it was found that the estimated α value over a forest is directly related to the forest biomass. Explaining this fact, the authors stated that "*the increase of the order parameter with biomass is not surprising*", since "*high-resolution SAR can, to some extent, resolve tree structures*" which are known to have different σ^0. Therefore, the corresponding SAR images will not present homogeneously distributed data and the K distributions of small order parameters will describe these highly fluctuating values well. As the tree biomass increases and the forests become dense, *SAR images tend to become statistically uniform, and the order parameter increases. In the limit of very dense forests with very large biomass, the SAR images appear as a statistically homogeneous classical speckle pattern, which can be described by the K-distribution of very large order parameter* (Wang and Ouchi, 2005, page: 4342).

It is important to observe that images acquired by the 3 × 3 m high-resolution PI-SAR L Band system were used in Wang and Ouchi (2005). Therefore, the spatial inhomogeneity shown by the σ^0 of a homogeneous extended target (all forest) was explained by taking into account that in different resolution cells different combinations of scattering sources, (soil, soil + trunk, branch + leaves, etc.), all corresponding to the same extended target, can be dominant. Since these scattering sources interact differently with the incident electromagnetic wave, they will in

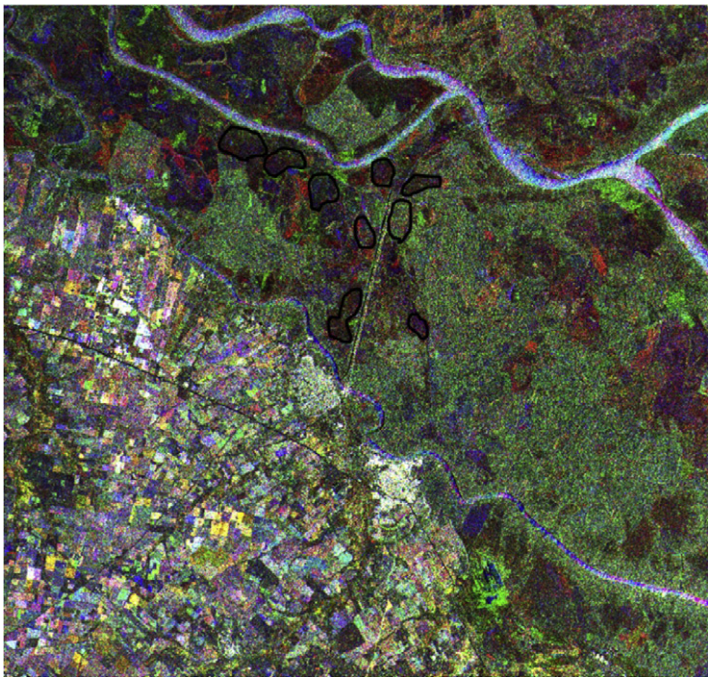

Fig. 1. Multitemporal Envisat ASAR image of the Lower Paraná River Delta. The *junco* marsh study areas are marked in black. Red: 04/03/2004, Green: 08/04/2004 and Blue: 13/05/2004. (For interpretation of the references to colour in this figure legend, the reader is referred to the web version of this article.)

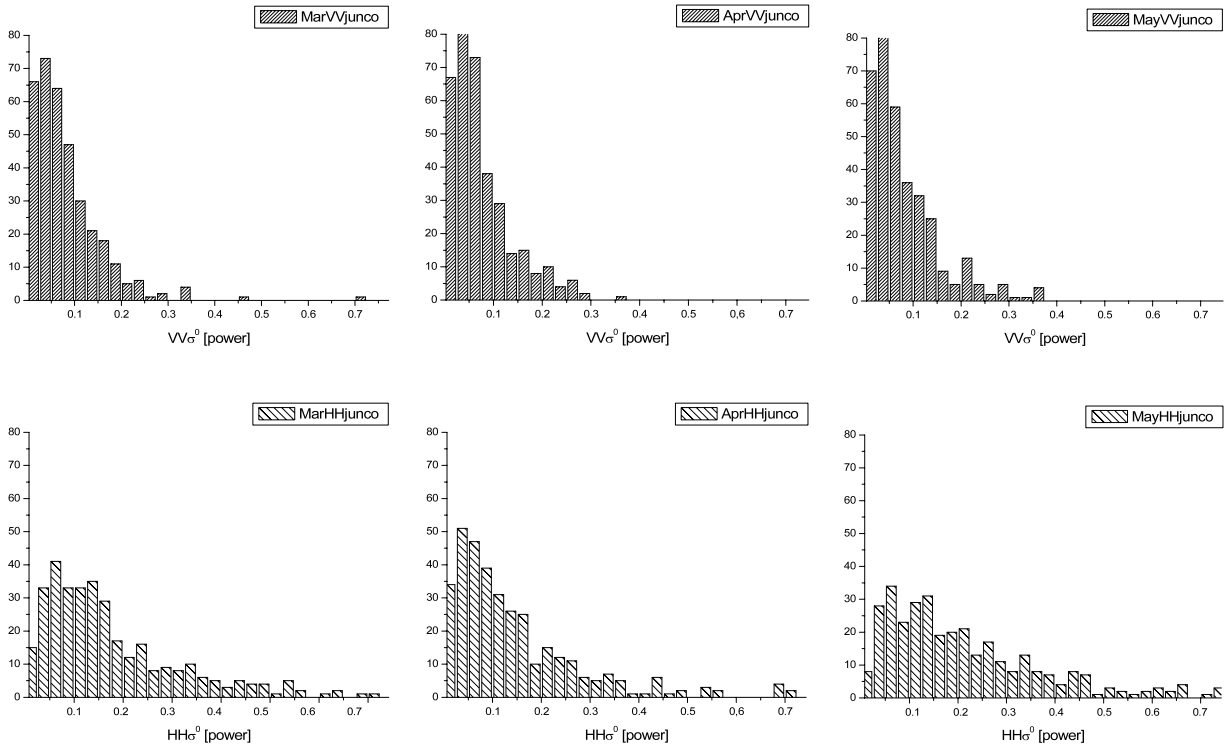

Fig. 2. σ^0 histograms extracted from ASAR images corresponding to *junco* samples. Top: VV polarization. Bottom: HH polarization. From left to right: 04/03/2004, 08/04/2004 and 13/05/2004.

general have different σ^0 values and the resulting distribution of the homogeneous area will present a small α value. When the biomass increases, the relative weight of the total σ^0 of the two target (i.e. soil and soil + trunk) combinations diminishes, and scattering from branches and leaves dominates. This leads to a high α value in the resulting distribution.

In our experimental data, we observed a similar phenomenon, at the C band and with two different vegetation structures. Our first observation is that forest samples present higher α values than *junco* samples. This result may be explained within the theoretical frame indicated above. At the L Band and for low biomass (Wang and Ouchi, 2005), a homogenous forest sample can be seen as an inhomogeneous area in an SAR image. However, at the C band (Envisat ASAR) a forest of almost any biomass will have a relatively high α value, since most of the electromagnetic energy will interact with the upper canopy. This is not the case for *junco* marshes,

Table 2
Estimated parameters for different dates, polarizations and vegetation types. The values are presented in decreasing order of α. *Junco* samples = 320, forest samples = 350. The distributions marked with an asterisk were rejected by the Kolmogov–Smirnov test (5% confidence level) as being K distributed.

ASAR acquisition parameters			Estimated parameters		
Date	Polarization	Target	α	β	Kolmogorov test p-value
Oct03*	VV	forest	68.6 ± 182	0.17 ± 2E–5	0.398
Apr04*	VV	forest	54.5 ± 280	0.19 ± 2E–5	0.156
Jan05*	HH	*Junco*	37.4 ± 16	0.09 ± 4E–4	0.260
Nov03*	VV	forest	36.6 ± 125	0.15 ± 2E–6	0.189
Mar04	VV	forest	19.4 ± 0.6	0.16 ± 2E–7	0.018
May04	HH	forest	16.8 ± 0.4	0.12 ± 8E–8	0.015
Jan05*	VV	forest	14.0 ± 291	0.16 ± 2E–5	0.165
Dec04	VV	forest	12.7 ± 0.4	0.17 ± 2E–7	0.019
Oct03	VV	*Junco*	12.2 ± 0.4	0.16 ± 2E–7	0.017
May04	VV	forest	11.7 ± 0.4	0.16 ± 2E–7	0.024
Apr04	VV	*Junco*	11.4 ± 0.4	0.07 ± 4E–8	0.011
Jan05	HH	forest	9.1 ± 0.4	0.13 ± 2E–7	0.029
Jan05	VV	*Junco*	7.9 ± 0.4	0.07 ± 8E–8	0.011
Dec04	HH	forest	7.2 ± 0.5	0.14 ± 4E–7	0.016
May04	VV	*Junco*	6.7 ± 0.5	0.08 ± 5E–7	0.028
Nov03	VV	*Junco*	6.4 ± 0.5	0.14 ± 5E–7	0.058
Mar04	HH	forest	6.2 ± 0.5	0.16 ± 7E–7	0.066
Mar04	VV	*Junco*	5.6 ± 0.5	0.08 ± 3E–7	0.051
Dec04	VV	*Junco*	5.0 ± 0.5	0.09 ± 4E–7	0.018
Nov03	HH	forest	4.5 ± 0.6	0.15 ± 2E–6	0.029
Apr04	HH	forest	4.1 ± 0.6	0.13 ± 2E–6	0.029
Nov03	HH	*Junco*	3.4 ± 0.6	0.44 ± 2E–5	0.011
Oct03	HH	forest	3.1 ± 0.7	0.17 ± 5E–6	0.029
Mar04	HH	*Junco*	3.0 ± 0.7	0.20 ± 8E–6	0.057
Apr04	HH	*Junco*	2.7 ± 0.7	0.15 ± 6E–6	0.029
Oct03	HH	*Junco*	2.4 ± 0.8	0.58 ± 8E–5	0.060
May04	HH	*Junco*	2.4 ± 0.8	0.26 ± 2E–5	0.056
Dec04	HH	*Junco*	1.0 ± 0.4	0.19 ± 7E–5	0.032

where the wave penetrates more easily down to the underlying water where the spatial distribution of water and nutrients can lead to a spatially inhomogeneous distribution of plant density (Keedy, 2000; Novitzki and Fretwell, 2002; Parmuchi et al., 2002). Taking into account that plant density is one of the variables that influence the *junco* σ^0 (Grings et al., 2006; Pope et al., 1997), it is not surprising that *junco* samples present a higher inhomogeneity (lower α values) than forests.

Furthermore, we observe that, in general, VV polarization presents higher α values than HH polarization. For the case of *junco*, this result may be explained as a consequence of the dominant scattering source (i.e. water/vegetation double bounce) and its polarization properties. This aspect will be discussed in the next section, with the aid of model simulation results.

Therefore, we can say: (1) that the majority of the ASAR samples (non-extreme environmental events) extracted on forest and *junco* marshes of the Paraná River Delta can be considered as $K(\alpha, \beta, n)$ distributed, (2) that the α parameter is different for different vegetation types and polarizations, and (3) that these differences can be interpreted by carefully analyzing the samples, the auxiliary data and the available fieldwork.

5. The interaction model

As we pointed out before, the inhomogeneity observed in the σ^0 of an extended target should be related to the spatially inhomogeneous distribution of a biophysical variable. In the case of *junco* marsh, it has been shown that the σ^0 of *juncos* over a flooded soil depends on a few biogeophysical variables (Grings et al., 2006). They are: *junco* shoot height, *junco* plant density, *junco* shoot radius, *junco* gravimetric water content, *junco* tilt angle distribution and *junco* dry matter density (Grings et al., 2006). Of all these variables, the only one that is known to change spatially is the *junco* plant density (JPD, m^{-2}). Recent fieldwork showed that the JPD distribution is not uniform inside a single marsh, and the density values change with a correlation length of 50 to 100 m. Considering that the ASAR APP pixel dimension is 12.5 m, this change in the JPD has a correlation length larger than the one expected for the speckle. As was mentioned before, inhomogeneity of the JPD is not uncommon in wetlands. Considering all this, our first hypothesis is that the observed σ^0 target variability is related to plant density spatial variability, and that the α parameter is able to map this inhomogeneity.

Our second hypothesis is that a model that is able to simulate the mean σ^0 of a *junco* marsh patch given the correct environmental conditions should also be able to simulate the σ^0 patch distribution given the JPD distribution as an input. In order to test this assumption we use the electromagnetic model described in detail in Bracaglia et al. (1995). This model was adapted to simulate the average values of *junco* marsh σ^0 in Grings et al. (2005, 2006, 2008, 2009). Basic information about the simulation procedure is summarized below.

The radiative transfer model

The backscattering coefficient was simulated using the multiple scattering model described by Bracaglia et al. (1995). The main steps, as well as the specific aspects related to *juncos*, are summarized below.

1. The medium is described as a lower half-space overlaid by discrete dielectric elements (Fig. 3). The lower half-space represents soil or water, depending on the flood conditions. *Junco* marshes are always flooded, although the water level may suffer variations. Therefore, the permittivity of the lower half-space is equal to the water permittivity. The discrete dielectric elements represent vegetation.
2. *Junco* shoots are described as dielectric cylinders under the "infinite length" approximation (Karam and Fung, 1988). The height and the orientation of the cylinders are assumed to vary within given ranges of values, according to statistical distributions derived by ground measurements (see Table 3). The extinction and bistatic scattering cross sections are computed, and then discretized by means of a matrix representation.

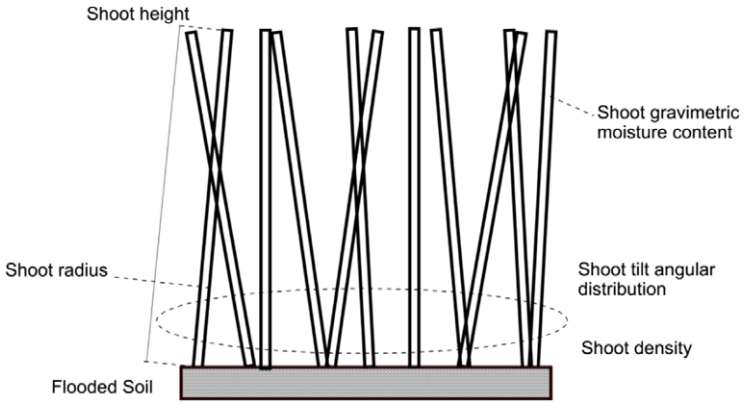

Fig. 3. Sketch of *junco* marsh architecture derived from fieldwork. The model uses this architecture and radiative transfer theory to simulate the σ^0 of the *junco* marsh.

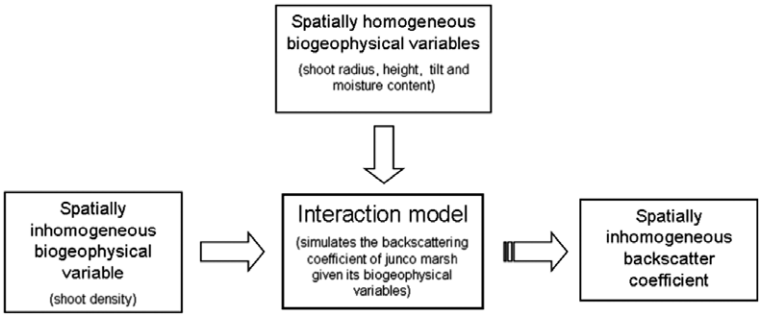

Fig. 4. Scheme of the adopted simulation procedure.

Table 3
Input variable mean values.

Junco marsh biogeophysical variable	value
Shoot height	180 ± 15 cm
Radius at 50 cm	0.35 ± 0.03 cm
Gravimetric moisture content	0.7 ± 0.05 g/g
Angular distribution	0–10 deg uniform
Dry matter density	0.15 ± 0.03 g/cm^3
Surface RMS height (flooded soil)	0.1 cm
Surface correlation length (flooded soil)	10 cm

3. The previously computed matrices represent scattering and extinction due to single elements at all incidence and scattering angles. Then, the effects of single vegetation elements are combined by using a numerical matrix algorithm.
4. Overall vegetation matrices are combined with soil (or water) matrices, using the same numerical algorithm. The scattering matrix of the overall medium is so obtained.
5. The backscattering coefficient may be computed by the scattering matrix, for the required incidence angle and polarization.

Details of the procedure are available in Bracaglia et al. (1995). The last three steps are carried out for several values of shoot density, and statistical averaging is finally applied.

We have used two sets of input variables: (1) SAR variables and (2) biogeophysical variables. The SAR variables are related to the system, and are the radar central frequency and the incidence angle (19° for ASAR APP S1 mode). The biogeophysical inputs are: shoot mean height (m), shoot mean diameter (cm), shoot orientation (degrees) and the statistical distribution of shoot density (m^{-2}). A summary of these is given in Table 3. The shoot permittivity is computed as a function of the moisture and the dry matter density using the empirical model given by El-Rayes and Ulaby (1987).

Since we state that the only variable that changes spatially is the *junco* plant density, our hypothesis is that all the observed inhomogeneities in the σ^0 should be related to the distribution of this variable. To test this hypothesis, we simulated the backscattering of a patch of *junco* marshes. All the biogeophysical parameters that characterize the environmental conditions are fixed or change with small correlation lengths, except the plant density d, which is Gaussian distributed in the sample, $d \sim N(\mu, \sigma)$. The assumption of a Gaussian distribution is based on available fieldwork over *junco* marshes. Fig. 4 shows the adopted procedure. To obtain a meaningful simulation, it is imperative to specify the numerical values of the other biogeophysical variables that determine the *junco* marsh σ^0. These values were obtained from the fieldwork available and are given in Table 3.

The key process in this simulation is the interaction model. In previous works, we used this model to simulate the σ^0 of *junco* for different environmental conditions, given the *junco* marsh biogeophysical variables as input. Now, we want to use the same model not only to predict a single σ^0 value, but the distribution of σ^0 values of a *junco* patch given as input (1) all the spatially homogeneous biogeophysical variables (shoot radius, height, tilt and moisture content) and (2) the spatially heterogeneous JPD distribution inside the patch.

Once we fix all the spatially homogeneous *junco* marsh biogeophysical variables, the *junco* marsh σ^0 is only a function of JPD. Therefore, there is a pair of "model transfer functions", one for each polarization, which transforms the JPD values into σ^0 values.

These transfer functions for the VV and HH polarizations are shown in Fig. 5. Both trends start with very low backscattering for zero density, since the direct backscattering of the flat water surface is very low. Then, the trends show a maximum for the density that maximizes the relation between the *junco* soil–shoot double bounce and the *junco* marsh extinction coefficient (different for different polarizations; see (Grings et al., 2005)) and finally the trend decreases monotonically, as expected when extinction dominates over backscattering.

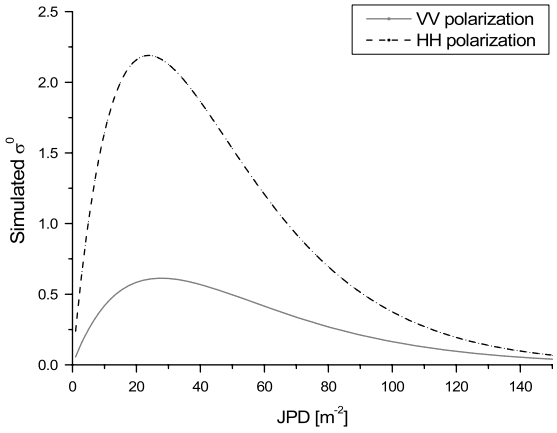

Fig. 5. Simulated σ^0 of *junco* marsh as a function of the JPD for VV (solid) and HH (dashed) polarizations. These functions can be thought of as the transfer functions of the radiative transfer interaction model.

6. Interaction model simulation results

Fig. 6 shows some of the simulated *junco* marsh σ^0 distributions, for a condition in which the input JPD values were Gaussian distributed. It can be seen that we have different simulated distributions for different marsh patch conditions, where the mean JPD and the JPD standard deviation define every patch condition.

In general, it can be seen that higher values of the JPD mean produce lower values of mean backscattering (β). This result is expected, since we are operating in the decreasing part of the model transfer function in Fig. 5. Also, the function is wide when the SD is large. This is also expected, since a wider input distribution corresponds to a wider output distribution. Next, we fitted the simulated data shown in Fig. 6 to a Gamma distribution $\Gamma(\alpha, \beta)$, in order to check if the hypothesis of a Gamma-distributed backscatter was a wise one. Table 4 presents the results of the fitting process.

From Table 4 and Fig. 6, two main considerations can be extracted. To first order, β is inversely proportional to the JPD mean, and α is inversely proportional to the JPD SD. The first result is not unexpected, since the *junco* σ^0 is known to decrease

Table 4
Estimated Gamma parameters (α, β) for VV and HH polarizations as a function of the JPD mean and JPD SD. The residual standard error, defined as sqrt($\Sigma_i(x_i - y_i)^2$/nsamples), is also given.

JPD mean	JPD SD	VV			HH		
		α	β	RMS	α	β	RMS
50	10	39.36	0.51	0.0756	20.74	1.57	0.0507
50	15	18.18	0.51	0.0798	9.82	1.64	0.0537
50	20	10.74	0.52	0.0835	6.24	1.69	0.0563
50	25	7.03	0.51	0.0872	4.31	1.70	0.0588
60	10	26.88	0.42	0.0907	15.95	1.24	0.0612
60	15	12.20	0.43	0.0804	7.19	1.28	0.0537
60	20	7.27	0.44	0.0845	4.26	1.35	0.0568
60	25	4.94	0.45	0.0886	2.97	1.40	0.0595
70	10	21.59	0.34	0.0924	13.41	0.95	0.0623
70	15	9.72	0.35	0.0961	6.16	0.98	0.0648
70	20	5.64	0.36	0.0849	3.61	1.02	0.0568
70	25	3.82	0.38	0.0894	2.47	1.08	0.0600
80	10	18.50	0.27	0.0937	11.91	0.71	0.0630
80	15	8.42	0.28	0.0977	5.53	0.73	0.0657
80	20	4.89	0.29	0.1016	3.29	0.77	0.0685
80	25	3.28	0.30	0.0894	2.26	0.81	0.0600
90	10	16.56	0.22	0.0943	10.93	0.53	0.0632
90	15	7.58	0.22	0.0987	5.11	0.54	0.0663
90	20	4.44	0.23	0.1028	3.07	0.57	0.0693
90	25	3.00	0.24	0.1069	2.13	0.60	0.0723
100	10	15.23	0.17	0.0756	10.23	0.39	0.0507
100	15	7.01	0.17	0.0798	4.81	0.40	0.0537
100	20	4.14	0.18	0.0835	2.92	0.42	0.0563
100	25	2.81	0.18	0.0872	2.04	0.44	0.0588
110	10	14.27	0.13	0.0907	9.72	0.28	0.0612
110	15	6.60	0.13	0.0804	4.59	0.29	0.0537
110	20	3.91	0.14	0.0845	2.80	0.30	0.0568
110	25	2.67	0.14	0.0886	1.98	0.32	0.0595
120	10	13.54	0.10	0.0924	9.32	0.20	0.0623
120	15	6.28	0.10	0.0961	4.42	0.21	0.0648
120	20	3.74	0.10	0.0849	2.71	0.22	0.0568
120	25	2.57	0.11	0.0894	1.92	0.23	0.0600
130	10	12.97	0.07	0.0937	9.00	0.14	0.0630
130	15	6.03	0.08	0.0977	4.28	0.15	0.0657
130	20	3.61	0.08	0.1016	2.64	0.15	0.0685
130	25	2.49	0.08	0.0894	1.88	0.16	0.0600

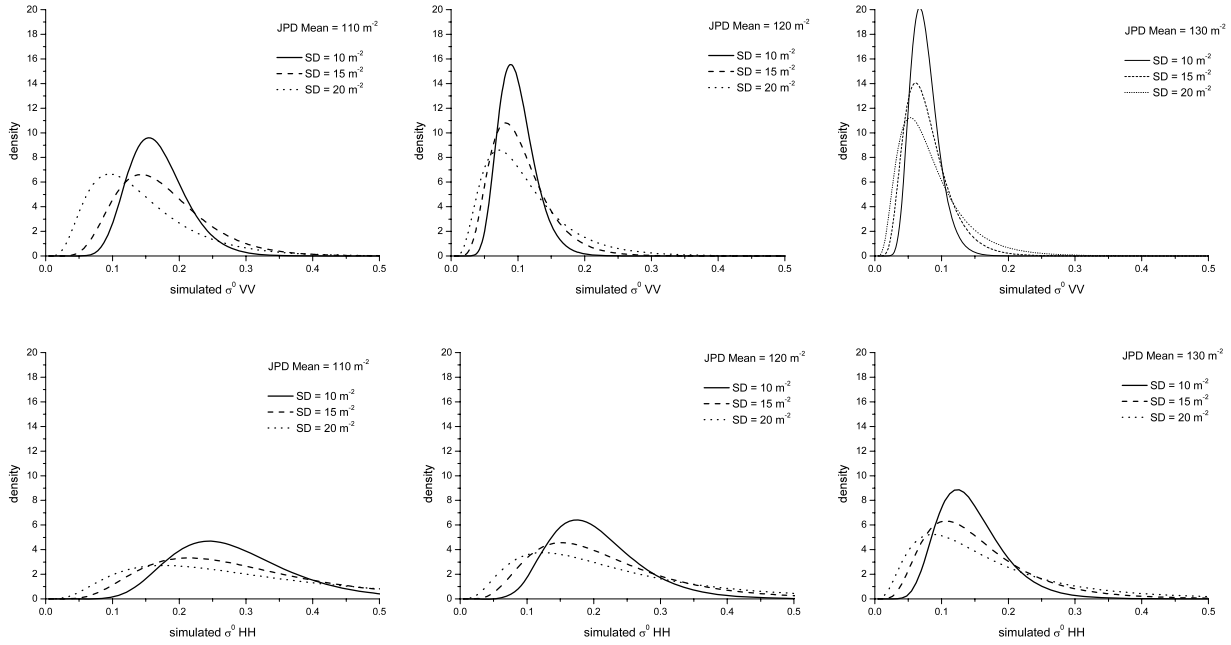

Fig. 6. Simulated *junco* marsh σ^0 distributions for different JPD distributions, characterized by the JDP mean value (JPD) and its standard deviation (SD). Top: VV polarization; bottom: HH polarization.

Table 5
α and β parameters estimated (left) from model simulations and (right) from ASAR images. The simulations were carried out taking as input the values of the *junco* marsh biogeophysical variables given in Table 3 and in the second and third columns of this table.

ASAR acquisition date	Fieldwork		Model simulation				Estimation from ASAR images			
	JPD mean	JPD SD	VV		HH		VV		HH	
			α	β	α	β	α	β	α	β
Mar/04	120	16	5.57	0.10	3.94	0.21	5.6 ± 0.5	$0.08 \pm 3E{-}7$	3.0 ± 0.7	$0.20 \pm 8E{-}6$
Apr/04	130	14	6.85	0.07	4.84	0.14	11.4 ± 0.4	$0.07 \pm 4E{-}8$	2.7 ± 0.7	$0.15 \pm 6E{-}6$
May/04	115	18	4.60	0.12	3.28	0.25	6.7 ± 0.5	$0.08 \pm 5E{-}7$	2.4 ± 0.8	$0.26 \pm 2E{-}5$

when the JPD increases for relatively large values of JPD ($>$ 50 plants/m^{-2}) (Grings et al., 2005). As we stated before, the inverse relation between α and the JPD SD can be explained by considering that a wider JPD input distribution, related to a high heterogeneity inside the marsh, leads to a wide dynamic range of simulated σ^0 values, corresponding to a small α value (remember that α increases with increasing homogeneity).

In summary, we can say: (1) that the assumption of the backscatter distributed $X \sim \Gamma(\alpha, \beta)$ agrees with fieldwork and numerical simulations carried out with an already tested interaction model of *junco* marsh, (2) that the hypothesis that the observed inhomogeneity is related to the spatial distribution of JPD is also sound, and (3) that for a given *junco* marsh environmental condition, the α and β parameters are inversely related to the JPD distribution parameters, the JPD mean and JPD SD, respectively.

7. Comparison of ASAR observations with fieldwork and model simulations

In this section we compare the estimated values of the α parameter from ASAR images with the model-simulated ones. As we said, to simulate the α parameter of a *junco* patch, it is necessary to provide all the biogeophysical parameters that define the σ^0 of the *junco* patch. All these parameters were already measured simultaneously with some of the ASAR acquisitions. However, to characterize the *junco* patch it is crucial to measure the JPD SD. This parameter is difficult to estimate, because to obtain a single meaningful value for a marsh patch it is mandatory to measure the JPD in numerous sites separated by tens of meters (remember that the JPD is the only biogeophysical variable that is spatially non-uniformly distributed). All these reasons limited the availability of field measurements of the JPD SD to three ASAR acquisitions. For these dates, it was possible (i) to estimate the α and β parameters from ASAR images and (ii) to simulate the α and β parameters using the RT transfer model presented in Section 5 using simultaneous field data as input. The results are summarized in Table 5.

It can be seen that there is a general agreement between the estimated and simulated statistical parameters. The good agreement between estimated and simulated β (mean σ^0) values was observed before (Grings et al., 2006, 2008), and is one of the cornerstones for the use of this interaction model to simulate the *junco* marsh radar response. The comparison between estimated and simulated α is also good for most of the samples. This implies that, to some extent, our simulation scheme is able to map the observed σ^0 inhomogeneity to the JPD spatial inhomogeneity.

However, there is a major discrepancy in the estimation of the α parameter for the April/04 acquisition (especially for VV polarization). The discrepancy is obviously not related to the fieldwork, since the measured values of the JPD mean and JPD SD for April/04 are similar to those of the other dates. This is expected, since the dates are very close and correspond to the same season (southern hemisphere autumn). Since the fieldwork data are similar, the simulated α and β values are also similar to those for the other dates. In view of the fact that the fieldwork and simulated data are consistent, the problem is not in the interaction model. Actually, the simulation scheme predicts that the observed α value for April/04 should be related to a JPD distribution with a much lower SD than the observed one. Consequently, there is another biogeophysical variable besides the JPD SD (such as a different flood or wind condition), that is inducing a very inhomogeneous σ^0 distribution.

8. Summary and conclusions

In this work, we have presented results of the relation between the K-distribution order parameters of the *junco* marsh σ^0 distribution and *junco* plant density statistical parameters. The results are based on the texture analysis of available Envisat ASAR data acquired between October 2003 and January 2005 over the Lower Paraná River Delta, Argentina. In order to extract useful information from the SAR data, a series of hypotheses was adopted:

- The multiplicative model can be used to model the SAR return (Oliver and Quegan, 1998).
- In the multiplicative model, the backscattering was assumed to follow a $X \sim \Gamma(\alpha, \beta)$ distribution and the speckle to assume a $Y \sim \Gamma(n, n)$ distribution (Lee et al., 1994; Oliver and Quegan, 1998).
- In *junco* marshes, the only biogeophysical variable that changes in the dimension of the ASAR pixel is the *junco* plant density.
- The radiative transfer based interaction model developed in Grings et al. (2005) and refined in Grings et al. (2006, 2008) can simulate the backscattering of *junco* marshes for different environmental conditions and polarizations.

Using these hypotheses, we have shown that Envisat ASAR APP samples of forest and *junco* marshes extracted over the Paraná River Delta can be considered as distributed $K(\alpha, \beta, n)$. This seems to be a general result, except when extreme environmental conditions (drought and floods) are observed, when the data cannot be considered as K distributed. Furthermore, we showed that the α parameter is different for different vegetation types and polarizations. This result was discussed in Section 4, and was previously mentioned by other authors for different vegetation structures and ecosystems (Oliver and Quegan, 1998; Wang and Ouchi, 2005). Also, the observed differences in the α parameter were successfully explained using environmental data.

To understand the observed results, we introduced an interaction model to simulate the distribution of σ^0 of *junco* marshes. We showed that the assumption of the backscatter distributed $X \sim \Gamma(\alpha, \beta)$ agrees with both the ASAR data and simulations carried out using available fieldwork. This is an interesting result, showing that a radiative transfer model is not only capable of simulating the mean σ^0 of a vegetated area, but also its order parameter. In this way, this work points out a possible link between statistical modeling and interaction modeling.

References

Alsdorf, D.E., 2002. Interferometric SAR observations of water level changes: Potential targets for future repeat-pass AIRSAR missions. In: AIRSAR Earth Science and Application Workshop, http://airsar.jpl.nasa.gov/documents/workshop2002/papers/H6.pdf (Accessed 25. 08. 09).

Arihood, B.E., Sidle, W., 2006. Hydrologic characteristics of a managed wetland and a natural riverine wetland along the Kankakee River in northwestern Indiana. Technical report. US Geological Survey Scientific Investigations Report, Report Number: 2006–5222, p. 78.

Blacknell, D., 1994. Comparison of parameter estimators for *K*-distribution. IEEE Proceedings on Radar, Sonar & Navigation 141 (I), 45–52.

Bracaglia, M., Ferrazzoli, P., Guerriero, L., 1995. A fully polarimetric multiple scattering model for agricultural fields. IGARSS, 1995, Quantitative remote sensing for science and applications: Congress Center, Firenze, Italy, 10–14 July 1995, by International Geoscience and Remote Sensing Symposium. 2 pp. 1339–1345.

Coe, M., 2000. Modelling terrestrial hydrological systems at the continental scale: Testing the accuracy of an atmospheric GCM. Journal of Climate 13 (4), 686–704.

Cribari-Neto, F., Frery, A.C., Silva, M.F.F., 2002. Improved estimation of clutter properties in speckled imagery. Computational Statistics and Data Analysis 40 (4), 801–824.

Jakeman, E., Pusey, P., 1976. A model of non-Rayleigh sea echo. IEEE Transactions of Antennas and Propagation 24 (6), 806–814.

El-Rayes, M.A., Ulaby, F.T., 1987. Microwave dielectric spectrum of vegetation - Part I: Experimental observations. IEEE Transactions on Geoscience and Remote Sensing GE 25 (5), 541–549.

Frery, A., Muller, H., Yanasse, C., Sant Anna, S., 1997. A model for extremely heterogeneous clutter. IEEE Transactions on Geoscience and Remote Sensing 35 (3), 648–659.

Grings, F., Ferrazzoli, P., Karszenbaum, H., Tiffenberg, J., Kandus, P., Guerriero, L., Jacobo-Berrles, J., 2005. Modeling temporal evolution of junco marshes radar signatures. IEEE Transactions on Geoscience and Remote Sensing 43 (10), 2238–2245.

Grings, F., Ferrazzoli, P., Jacobo-Berlles, J., Karszenbaum, H., Tiffenberg, J., Pratolongo, P., Kandus, P., 2006. Monitoring flood condition in marshes using EM models and Envisat ASAR observations. IEEE Transactions on Geoscience and Remote Sensing 44 (4), 936–942.

Grings, F.M., Ferrazzoli, P., Karszenbaum, H., Salvia, M., Kandus, P., Jacobo-Berlles, J.C., Perna, P., 2008. Model investigation about the potential of C band SAR in herbaceous wetlands flood monitoring. International Journal of Remote Sensing 29 (17-18), 5361–5372.

Grings, F.M., Salvia, M., Karszenbaum, H., Ferrazzoli, P., Kandus, P., Perna, P., 2009. Exploring the capacity of radar to estimate wetland marshes water storage. Journal of Environmental Management 90 (7), 2189–2198.

Järvelä, J., 2004. Flow resistance in environmental channels: Focus on vegetation. Helsinki University of Technology Water Resources Publications. Espoo 2004, TKK-VTR-10. http://lib.tkk.fi/Diss/2004/isbn9512270749/ (accessed 25. 08. 09).

Karam, M.A., Fung, A.K., 1988. Electromagnetic scattering from a layer of finite length, randomly oriented, dielectric, circular cylinders over a rough interface with application to vegetation. International Journal of Remote Sensing 9 (6), 1109–1134.

Keedy, P., 2000. Wetland Ecology. Principles and Conservation. Cambridge University press, Cambridge, UK, 614 pp. ISBN 0521783674, paperback.

Lee, J.S., Schuler, D.L., Lang, R.H., Ranson, K.J., 1994. *K*-distribution for multilook processed polarimetric SAR imagery. Geoscience and Remote Sensing Symposium, 1994. IGARSS'94. Surface and Atmospheric Remote Sensing: Technologies, Data Analysis and Interpretation 4 (8–12), pp. 2179–2181.

Nepf, H., Koch, E., 1999. Vertical secondary flows in submersed plant-like arrays. Limnology and Oceanography 44 (4), 1072–1080.

Novitzki, R.P., Fretwell, J., 2002. Restoration, Creation, and Recovery of Wetlands: Wetland Functions, Values, and Assessment. Technical report, United States Geological Survey Water Supply Paper 2425. http://water.usgs.gov/nwsum/WSP2425/functions.html (accessed 25. 08. 09).

Oliver, C., Quegan, S., 1998. Understanding Synthetic Aperture Radar Images. In: Artech House Remote Sensing Library. Artech House Publishers.

Parmuchi, M.G., Karszenbaum, H., Kandus, P., 2002. Mapping the Paraná River delta wetland using multitemporal RADARSAT/SAR data and a decision based classifier. Canadian Journal of Remote Sensing 28 (2), 175–186.

Pope, K.O., Rejmankova, E., Paris, F.F., Woodruff, R., 1997. Detecting seasonal flooding cycles in marshes of the Yucatan peninsula with SIR-C polarimetric radar imagery. Remote Sensing of Environment 59 (2), 157–166.

Richey, J.E., Mertes, L.A.K., Dunne, T., Victoria, R.L., Forsberg, B.R., Oliveira, E., 1989. Sources and routing of the Amazon river flood wave. Global Biogeochemical Cycles 3 (3), 191–204.

Stone, B, Hung, Tao Shen, 2002. Hydraulic resistance of flow in channels with cylindrical roughness. Journal of hydraulic engineering 128 (5), 500–506.

Wang, H., Ouchi, K., 2005. The relation between the order parameter of *K*-distribution in high-resolution polarimetric SAR data and forest biomass. In: Geoscience and Remote Sensing Symposium, 2005. IGARSS'05. Proceedings, vol. 6, 25–29 July 2005, pp. 4339–4342.

Yanasse, C.C.F., Frery, A.C., Sant'Anna, S.J.S., Dutra, L.V., 1994. On the use of multilook amplitude *K* distribution for SAR image analysis, In: Geoscience and Remote Sensing Symposium, 1994. IGARSS'94. Surface and Atmospheric Remote Sensing: Technologies, Data Analysis and Interpretation, International, vol. 4, 8–12 Aug, pp. 2173–2175.